JOURNAL OF Applied Polymer SCIENCE

Control of Well-Defined Crater Structures on the Surface of Biaxially Oriented Polypropylene Film by Adding Nucleators

Satoshi Tamura,[1] Toshitaka Kanai[2]
[1]Prime Polymer Co., Ltd., 580-30, Nagaura, Sodegaura-city, Chiba, 299-0265, Japan
[2]Idemitsu Kosan Co., Ltd., 1-1, Anesaki-Kaigan, Ichihara-city, Chiba, 299-0193, Japan
Correspondence to: T. Kanai (E-mail: toshitaka.kanai@si.idemitsu.co.jp)

ABSTRACT: While it is common to add anti-blocking agents to biaxially oriented polypropylene (BOPP) films for general use in order to prevent blocking against each other, the technology of crater-like film surface roughness formed on the BOPP films without any additives is well known in the industrial BOPP film areas. Numerous studies have been reported on the crater-like film surface roughness on the BOPP films since the 1980s, but its formation mechanism and the controlling method of the crater-like film surface roughness are yet to be clarified. In our previous reports, we presented a new hypothesis of crater formation mechanism from a new point of view on sheet morphology and crater shape on the BOPP film surface. It was strongly influenced by the crystal grain shape in the surface layer of PP sheet. In this report, it was clarified that a nucleator has a big influence on the formation of the crystal grains in the surface layer of PP sheets and on the formation of craters. In addition, craters did not form on the BOPP films stretched from the sheet of which the skin layer with crystal grain was shaved, even though β crystal still remained. It was clarified that the crystal grain is trans-crystal from the observation using TEM. Therefore, it is concluded that the existence of β crystals in the surface layer of PP sheets is not essential in order to produce craters on BOPP films, but trans-crystals are necessary to form the craters. © 2013 Wiley Periodicals, Inc. J. Appl. Polym. Sci. 130: 3555–3564, 2013

KEYWORDS: films; polyolefins; surfaces and interfaces

Received 11 February 2013; accepted 27 April 2013; Published online 26 June 2013
DOI: 10.1002/app.39472

INTRODUCTION

Polypropylene (PP) is one of the most widely used thermoplastic resins with semicrystalline structures. It is well known that PP has different crystal system such as α crystal (monoclinic), β crystal (hexagonal), γ crystal (orthorhombic), and smectic form. The α crystal is the most stable structure analyzed by Natta and Corradini in 1960.[1] The amount of α crystals increases by adding α nucleator such as PTBBA-Al (*p-tert*-butyl benzoic acid monohydroxy aluminum)[2] and phosphate compounds.[3] The β crystal is semi-stable system of crystal reported by Keith in 1959.[4] One of the pigments, γ quinacridone is the long-standing β nucleator,[2] and amide type compound is currently popular β nucleator.[5,6] It is reported that β crystal can be easily formed under a strong shear stress.[7] Farah et al.[8] reported that very small α crystal was formed on the external layer of PP sheet extruded by T-die because the crystallizing speed of α crystal is higher than that of β crystal at higher temperature over 140. Whereas the β crystals were formed at the second layer just under the external layer because the crystallizing speed of β is higher than that of α crystals at the temperature range from 100°C to 140°C. Nakamura et al.[9] also reported that the highest crystallizing speed of β crystal is 79°C and that of α crystal is 70°C.[9]

In addition to the various researches on the stretchability of the BOPP films,[10–19] the formation of crater-like surface roughness of BOPP films was also reported with the connection of crystal system. The β crystal has a lower density of 921 kg/m^3 and melting temperature of 148°C compared to those of α crystal of 936 kg/m^3 and 164°C, respectively. The β crystal in PP sheets which contain both α and β crystal changes into α crystal after stretching at the temperature range from 148°C to 164°C, which is the melting point of β crystal and α crystal, respectively.[20] Since the crater is formed when the β crystal part sinks because of its lower density compare to α crystal, it is reported that the crater-like surface roughness was caused by the crystal dislocation system using the difference of crystal density.[21–24] It is also reported that since the craters became unclear in roughened BOPP film at a lower temperature and the craters disappeared by melting at a higher temperature, the stretching temperature in the transverse direction (TD) should be controlled between 150°C and 155°C.[21] Furthermore, Fujiyama et al. reported the difference of the surface roughness between the BOPP film

Applied Polymer SCIENCE

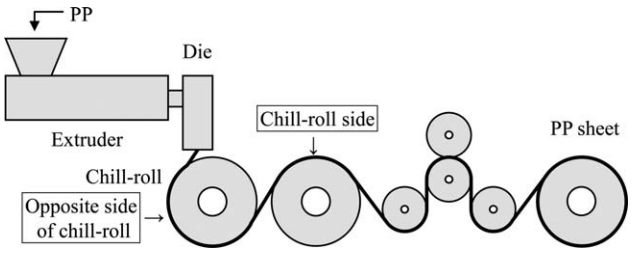

Figure 1. Schematic diagram of PP sheet forming machine.

produced by the sheet with α nucleator and that with β nucleator. In this report, in spite of the good relationship between the crater diameter and the β crystal diameter was reported, the amount of β nucleator and the surface roughness has not yet been clarified.[2] From these reports, the crater formation mechanism of BOPP films has not yet been clarified, because the previous reports solely focused on the β crystal.

We came up with a new hypothesis in our previous report[25] that the crater-like surface roughness on BOPP films was related to the morphology of the surface layer of the PP sheets.[26] We also reported that the surface roughness controlling system on the point of sheet and film producing condition.[27] This report will demonstrate a controlling system of film surface roughness by controlling the resin properties with the new α and β nucleators, and the crater formation mechanism by analyzing the morphology of PP sheets.

EXPERIMENTAL

Samples

PP samples with α nucleator or β nucleator were prepared in order to clarify the influence of nucleator on the formation of the surface craters. 3-Methyl-1-butene was used as α nucleator and *N,N′*-dicyclohexyl-2,6-naphthalene dicarboxamide (NJSter NU-100 produced by New Japan Chemical Co.) was used as β nucleator.[5,6] The isotacticity parameter meso pentad values mmmm was measured by Carbon-13 Nuclear Magnetic Resonance [^{13}C-NMR, JOEL (Tokyo, Japan) RAMBDA] Spectroscopy.[28] Thermal properties of melting point (T_m), melting enthalpy (ΔH_m), and crystallization temperature (T_c) were measured by differential scanning calorimetry (DSC, PerkinElmer (Waltham, MA, B014-3018/B014-3003).

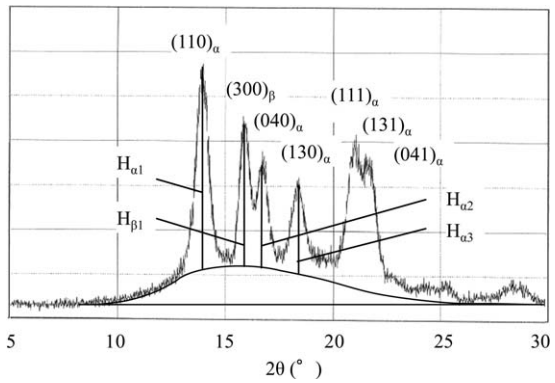

Figure 2. X-ray diffraction pattern of PP sheet and evaluation of β-form crystal ratio (*K* values).

PP sheets were produced using a sheet forming machine (GM Engineering, Yokohama, Japan) with φ = 35 mm extruder from a die with a width of 200 mm at 250°C (Figure 1). Then PP resins were cast by a chill-roll with a diameter of φ = 250 mm at 0.8 m/min at 80°C. After the PP sheets were cut into a square shape of 85 × 85 mm in size, the PP sheets were stretched by a table tender (Bruckner, Siegsdorf, Germany, KARO χ) in order to analyze the surface structure of BOPP films. BOPP film was stretched after PP sheet was pre-heated for 1 min at an arbitrary temperature at a maximum stretching ratio of five times to the machine direction (MD) and seven times to the transverse direction (TD). In this report, PP sheet samples were named in order of resin type, chill-roll temperature, thickness, whereas sample name of 'A0-80-500' means the sheet was made by PP-A0 at the chill-roll temperature of 80°C with thickness of 500 μm. The BOPP film names were defined by putting "f" at the end of PP sheet names, for example "A0-80-500f."

In order to clarify the crater formation mechanism more deeply, PP sheets produced by a pressing machine (SHINTO Metal Industries Corporation, Oosaka, Japan) were prepared to evaluate the influence of shear stress. After PP pellets were pressed in the mold whose size is 200 × 200 × 0.5 mm at the pressure of 50 kg f at 250°C for 5 min, PP sheets were formed by cooling at the pressure of 100 kg f at 80°C for 3 min. PP sheets were stretched by a table tenter at the same condition with PP sheet

Table I. Properties of Samples with Different Amount of α and β Nucleators

Properties		Units	A0	Aα1	Aα2	Aα3	Aα4	Aβ1	Aβ2	Aβ3	Aβ4
	Type	-	-	α	α	α	α	β	β	β	β
Nucleator	Content	ppm	-	10	30	100	300	10	30	100	300
DSC	T_m	°C	164.1	164.3	164.6	165.5	165.5	164.2	164.4	171.0	170.6
			148.5	149.2	149.8	150.0		148.6	155.1	152.4	167.4
									149.6		154.4
	ΔH_m	J/g	101.3	105.7	102.9	102.2	102.0	99.6	100.0	101.6	107.6
	T_c	°C	114.1	115.0	117.2	117.8	118.5	113.7	114.1	123.1	127.2
WAXD	χ_c	%	65	68	70	68	69	67	67	65	70
	K	-	0.09	0.00	0.00	0.00	0.00	0.09	0.09	0.15	0.88

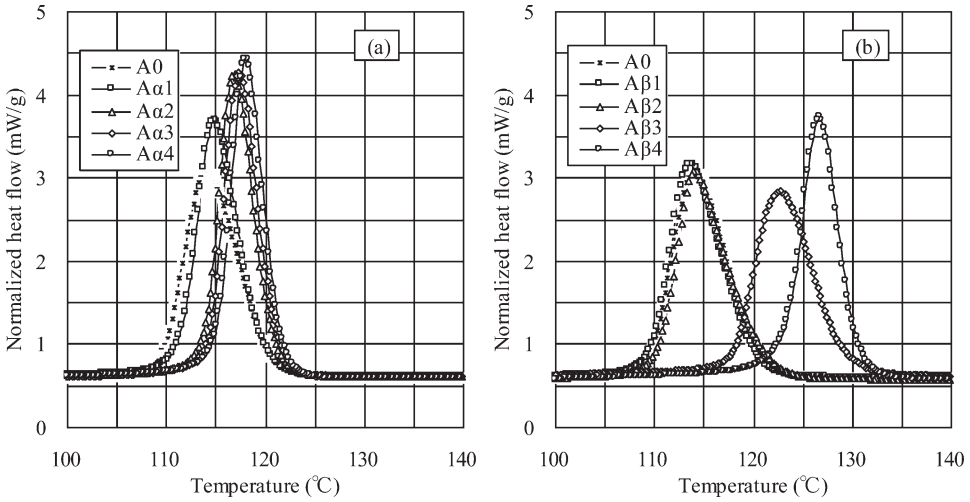

Figure 3. Cooling behavior of each PP with (a) α nucleator and (b) β nucleator measured by DSC.

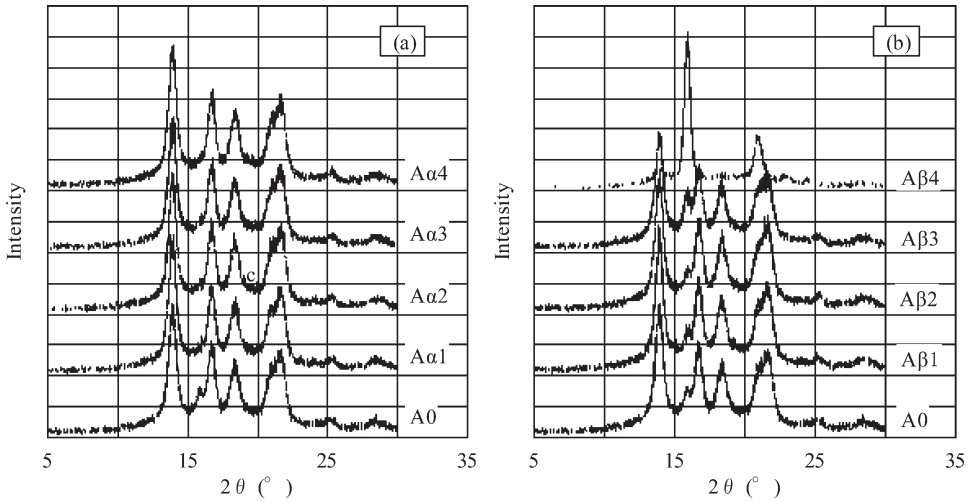

Figure 4. X-ray diffraction patterns of each PP sheet with (a) α nucleator and (b) β nucleator.

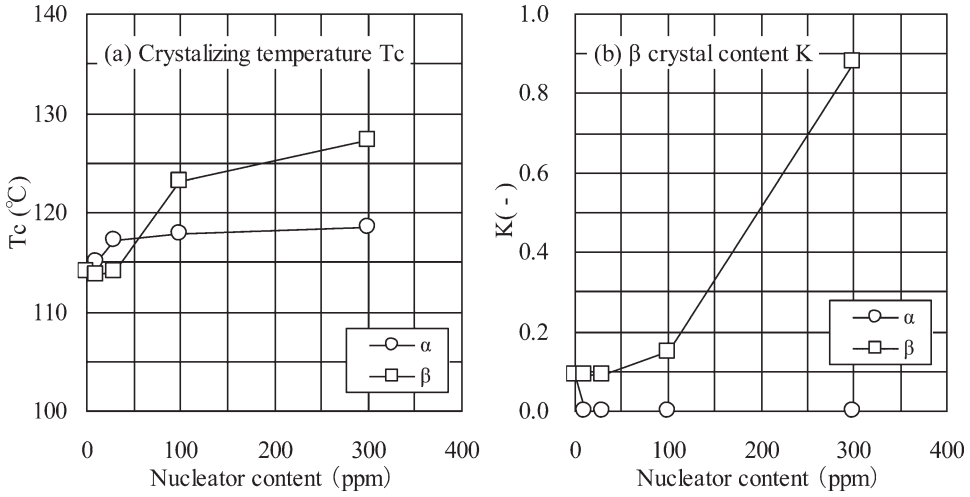

Figure 5. Properties of samples with different amount of α and β nucleators: (a) Tc and (b) *K*.

Applied Polymer SCIENCE

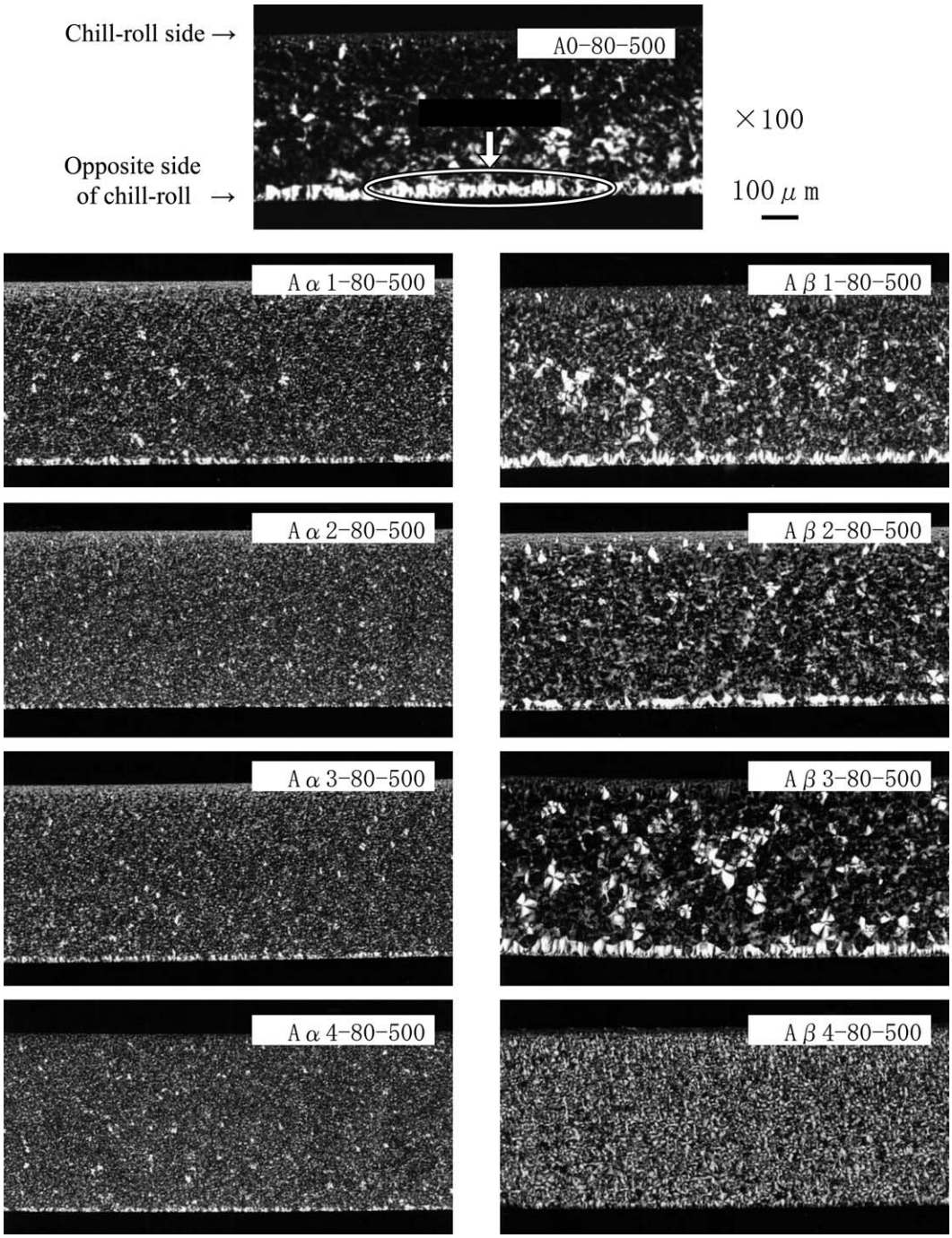

Figure 6. Optical microscope images of PP sheets with different amount of α and β nucleators.

produced by a sheet forming machine. PP sheet produced by a pressing machine and the BOPP film stretched from the sheet were named "A0-80P-500" and "A0-80P-500f." Furthermore, PP sheets whose surface layers were cut by SAICAS (DAIPLA WINTES Co., Saitama, Japan, DN-20S) were prepared in order to investigate the influence of the morphology of surface layers.

Evaluation of PP Sheets and the BOPP Films

The surface structure of BOPP films was observed by SEM (JOEL, Tokyo, Japan, JSM5600LV) sputtered with gold in a vacuumed condition. In addition, the shapes of the craters were measured by visual inspection from pictures taken with SEM and by a highly precise shape measuring machine (Kosaka Laboratory, Tokyo, Japan, SURFCODER ET4000A) using a diamond head at a head pressure of 70 μN. The sectional structures of PP sheets were observed by an optical microscope (Nikon, Tokyo, Japan, ECLIPSE-LV100POL) and TEM (Hitachi, Tokyo, Japan, H-7650). On observing the PP sheet sectional structure using an optical microscope, crystal sizes were measured by visual inspection from pictures taken with a polarizing

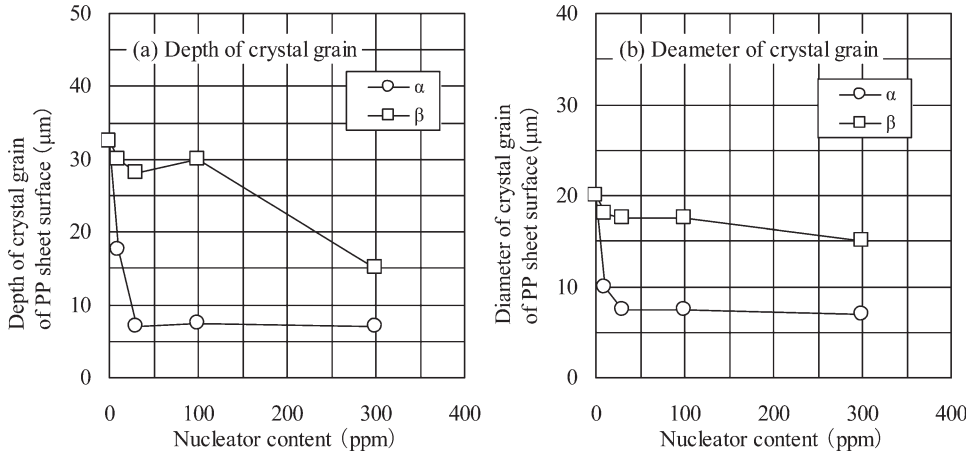

Figure 7. Crystal grain size of PP sheets with different amount of α and β nucleators.

lens. On observing the sectional structure using TEM, sample was dyed by osmium in order to divide high crystallinity parts from low crystallinity parts and was cut at the freezing condition after it was buried into epoxy resin.

X-ray diffractions were measured on the PP sheets with a Rigaku Denki (Tokyo, Japan) RINT-2500 diffractometer with Ni-filtered Cu *Kα* radiation. The *β* crystal content named as *K*-value was calculated from the diffraction curves shown in Figure 2 according to the *eq.* (1) proposed by Tuner Jones,[29] and crystallinity χ_C of PP sheets which is an index of the quantity of the crystal part was calculated from the diffraction curves according to the *eq.* (2) proposed by Giulio Natta.[30]

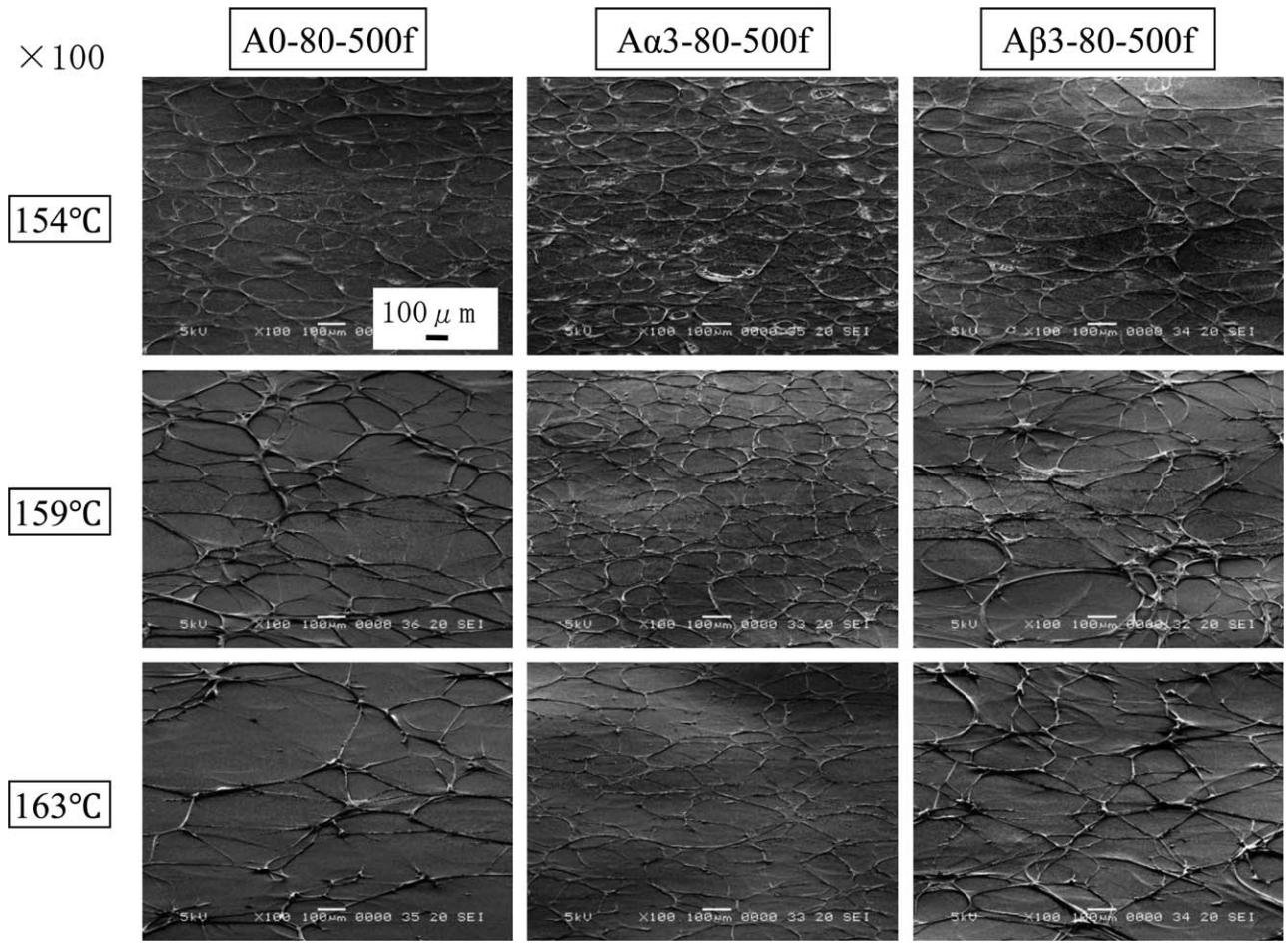

Figure 8. SEM image of the surface of the opposite side of chill-roll of PP film stretched from PP sheet with α and β nucleators.

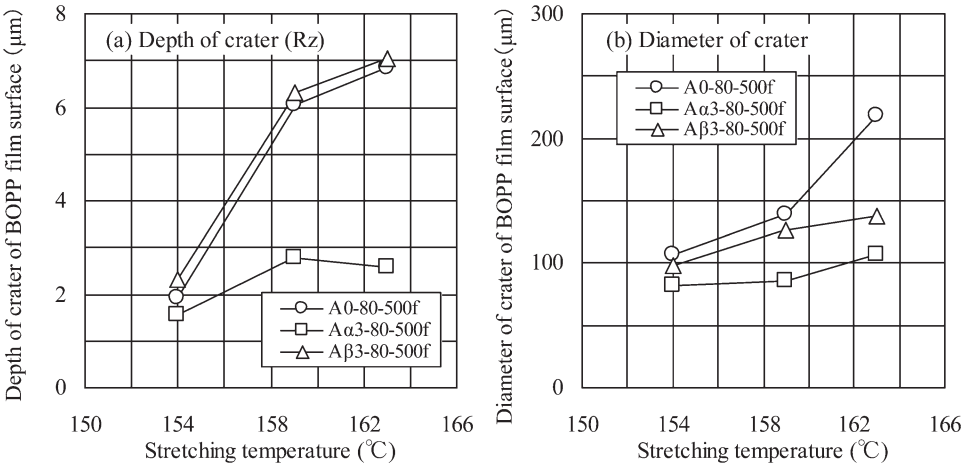

Figure 9. Surface structure of PP film stretched from PP sheet with α and β nucleators.

$$K=\frac{H\beta 1}{H\beta 1+H\ \alpha\ 1+H\ \alpha\ 2+H\ \alpha\ 3} \quad (1)$$

Where $H\beta1$, $H\alpha1$, $H\alpha2$, and $H\alpha3$ are the reflection intensities of the (3 0 0) plane of β crystals, (1 0 0), (0 4 0), and (1 3 0) planes of α crystals, respectively.

$$\chi_C=\frac{I_c}{I_c+6.21\times I_a} \quad (2)$$

Where I_c is the total area of crystal part and I_a is total area of amorphous part.

RESULTS AND DISCUSSION

The Influence of Nucleator on the Crater Formation of BOPP Film

At first, PP samples with different amount of nucleators were prepared in order to study the influence of the type of nucleator on the formation of a crater (Table I). Crystallizing behavior measured by DSC and X-ray diffraction patterns are shown in Figures 3 and 4, respectively. T_c, which is the factor showing the effect of nucleator most notably, increased remarkably when more than 30 ppm of α nucleator and more than 100 ppm of β nucleator were added to PP resin [Figures 3 and5(a)]. Although β crystal content *K*-value of PP sheet fell down less than 1% which is the lower limit of detection when more than 10 ppm of α nucleator was added to PP resin. In the meantime, *K*-value of PP sheet with β nucleator increased when more than 100 ppm of β nucleator was added to PP resin [Figures 4 and5(b)]. From these results, PP with nucleator amount of 100 ppm is mainly studied in order to clarify the influence of nucleator on the crater of BOPP films.

Figure 6 shows the MD and normal direction (ND) cross-sectional view of PP sheets with 100 ppm of nucleator compared to PP sheet without nucleator. Although the crystal grain size in the surface layer of the opposite side of chill-roll of PP sheet with 100 ppm of α nucleator (Aα3-80-500) became smaller than that of PP sheet without nucleator (A0-80-500), that of PP sheet with 100 ppm of β nucleator (Aβ3-80-500) was the same as that of PP sheet of A0-80-500. Figure 7 shows the relationship between the crystal grain size and the amount of nucleator. Both crystal grain depth and diameter of PP sheet with α nucleator became smaller than those without nucleator and were stable when more than 30 ppm of α nucleator was added to PP resin. Meanwhile, although crystal grain size of PP sheet with β nucleator less than 30 ppm was not changed, it became smaller

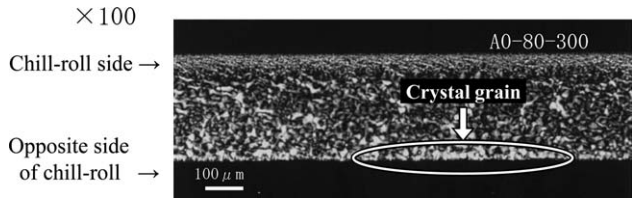

Figure 10. Optical microscope image of A0-80-300 sheet which was used to slice the surface layer of the opposite side of chill-roll. *Crystal grain depth: 26 μm.

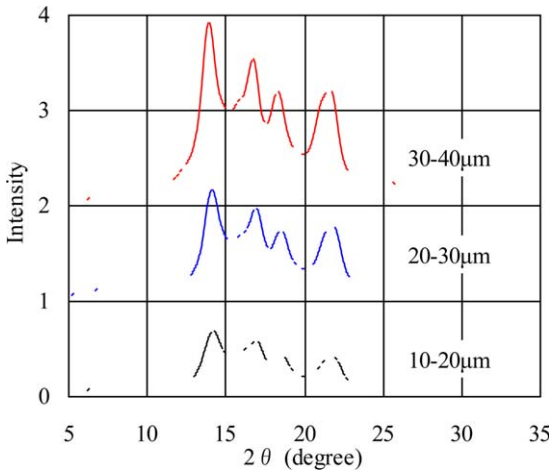

Figure 11. X-ray diffraction patterns of shaved chips of A0-80-300 sheet from the opposite side of chill-roll. *10–20 μm: shaved chip from the depth of 10–20 μm; *20–30 μm: shaved chip from the depth of 20–30 μm; *30–40 μm: shaved chip from the depth of 30–40 μm. [Color figure can be viewed in the online issue, which is available at wileyonlinelibrary.com.]

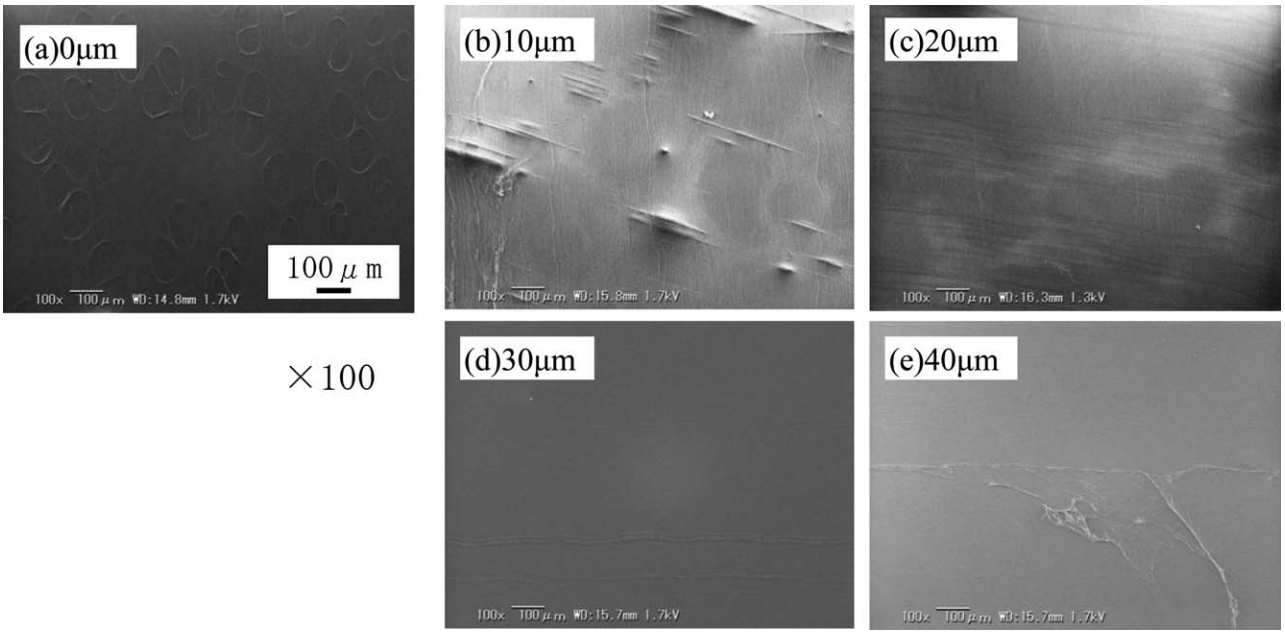

Figure 12. SEM image of the surface of A0-80-500f film stretched from non-shaved and shaved sheets from the surface of the opposite side of chill-roll. (a) Non-shaved sheet, (b) shaved for 10 μm, (c) shaved for 20 μm, (d) shaved for 30 μm, and (e) shaved for 40 μm.

when 100 ppm of β nucleator was added. The reason why β nucleator required more amount than α nucleator in order to get smaller size of crystal grain is that β nucleator is difficult to demonstrate its ability in the surface layer because β crystal is easy to form under the influence of shear stress.[7]

Figure 8 shows SEM images of surface of BOPP films with and without nucleator stretched at several stretching temperatures and Figure 9 shows a shape of crater. The crater shape of BOPP films with 100 ppm of α nucleator Aα3-80-500f became smaller than the one without nucleator A0-80-500f as it was expected from the crystal grain size of PP sheet. Although the crater of A0-80-500f became larger and deeper with the increase of the stretching temperature, the size of crater of Aα3-80-500f did not change notably at high stretching temperature. It is because the crystal grain size of Aα3-80-500 is smaller than that of A0-80-500. Meanwhile, although the crater depth of Aβ3-80-500f became larger with the increase of stretching temperature like that of A0-80-500f, the crater diameter did not change remarkably unlike that of A0-80-500f. The reason why the depth of crater of Aβ3-80-500f indicated the similar behavior with A0-80-500f was that the crystal grain size of Aβ3-80-500 was the same with that of A0-80-500. The diameter of crater of Aβ3-80-500f became smaller than that of A0-80-500f at high stretching temperature in spite of the same diameter of crystal grain. It is supposed that crater of A0-80-500f became larger by connecting each crater because the melting point of A0-80-500 was 165 and 6°C lower than that of Aβ3-80-500. From these results, the depth and diameter of crater can be controlled independently by adding the different type of nucleator and its amount.

The Influence of Morphology of Surface Layer on the Crater Formation of BOPP Film

Next, in order to investigate the influence of crystal grain in the surface layer of PP sheet on the crater of BOPP film surface, it was cut the surface layer of the opposite side of chill-roll of PP sheet A0-80-300 with the crystal grain depth of 26 μm by SAICAS (Figure 10). Figure 11 shows the WAXD pattern of shaved chip from the opposite side of chill-roll with every 10 μm depth. "10–20 μm" means the chip with the thickness of 10 μm shaved from the depth of 10–20 μm from the opposite side of chill-roll of the sheet. When the sheet was shaved from the opposite side of chill-roll to the depth of 40 μm every 10 μm, each shaved chip had β crystal more than K value of 0.2. Since the depth of crystal grain was 26 μm, there were different shapes of β crystal in the 30–40 μm layer. Figure 12 shows SEM images of BOPP films surface stretched from the PP sheets with surface layer shaved. Clear crater was observed on the BOPP film stretched from the PP sheet without shaving [Figure12 (a)], and crater like pattern was observed on the surface of BOPP film stretched from the PP sheet remained after shaving at the depth of 10 μm [Figure 12 (b)]. Meanwhile, crater was not observed on the BOPP films surface stretched from the PP sheets remained after shaving more than 20 μm [Figure 12(c–e)]. From these studies that there is a case when no crater on BOPP film surface forms from PP sheet with β crystal, it was clarified that crystal grain in the surface layer of PP sheet is necessary to form crater on BOPP film surface (Table II).

In order to clarify the influence of crystal grain of PP sheets on crater in BOPP films surface, sectional structure of opposite side of chill-roll of PP sheet was observed by TEM (Figure 13). There were characteristic grains in the layer of the depth from 2 to 20 μm different from the grains in the layers deeper than 20 μm. Since these characteristic grains seemed to grow from the depth of 2 μm to the depth direction, they are assumed to be trans-crystals grown from the skin layer as nuclei [Figure 13(a)]. From the MD and ND cross-sectional view of PP sheet stretched to MD at the stretching ratio of 1.2 [Figure 13(b)]

Applied Polymer SCIENCE

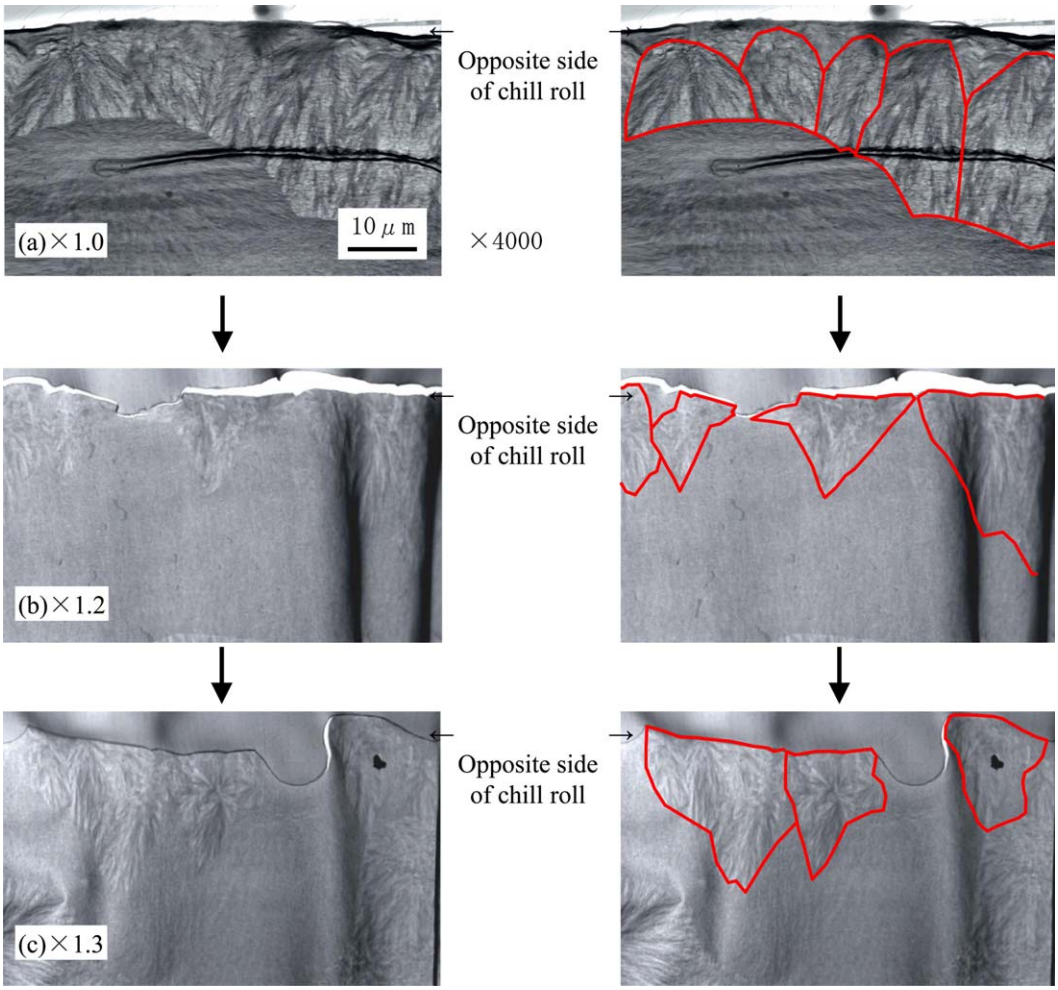

Figure 13. Cross sectional image of (a) non-stretched A0-80-500 sheet, (b) stretched at 1.2 times, and (c) stretched at 1.3 times observed by TEM. [Color figure can be viewed in the online issue, which is available at wileyonlinelibrary.com.]

and 1.3 [Figure 13(c)], apertures were observed between trans-crystals which were assumed to be the precursors of craters as was mentioned in our previous report.[25] From these results, it was concluded that crater was formed by the changing and deforming of trans-crystal starting with the apertures between the trans-crystals.

Furthermore, PP sheets produced by a pressing machine were prepared in order to investigate the influence of trans-crystals of

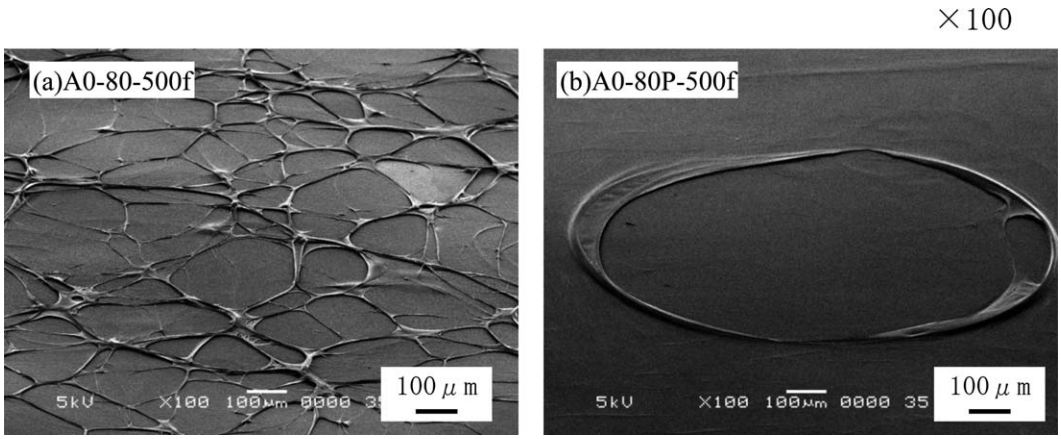

Figure 14. SEM image of the surface of the opposite side of chill-roll of (a) A0-80-500f film and (b) A0-80P-500f film.

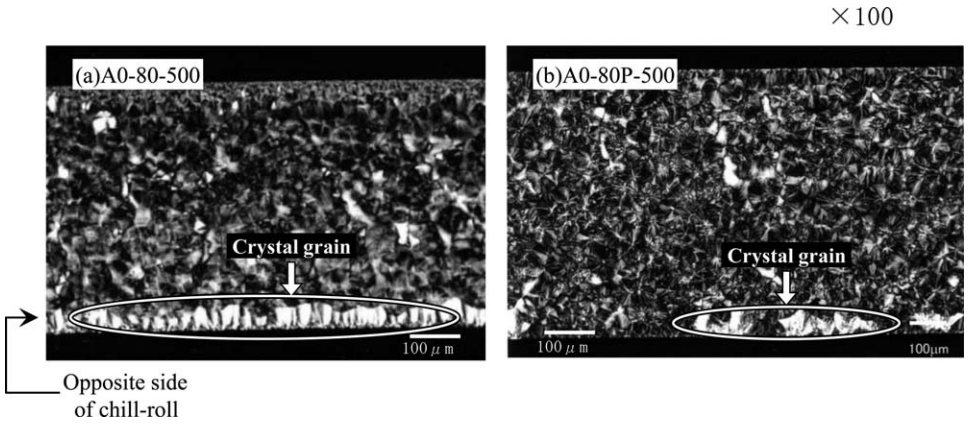

Figure 15. Optical microscope image of (a) A0-80-300 sheet and (b) A0-80P-500 sheet.

surface layer, compared with the PP sheet produced by a sheet forming machine. As a result, craters formed on the A0-80P-500f films stretched from PP sheet produced by a pressing machine were fewer and larger than those formed on the A0-80-500f films stretched from PP sheet produced by a sheet forming machine (Figure 14). In order to clarify the cause of the difference of crater formation between A0-80P-500f and A0-80-500f, the MD and ND cross-sectional structure of PP sheets were observed by OM (Figure 15). It was found that the trans-crystals formed in the surface layer of A0-80P-500 sheet were fewer and larger than those of A0-80-500. Consequently, the reason why the craters of A0-80P-500f film were fewer and larger than those of A0-80-500 is that the trans-crystals in the surface layer of A0-80P-500 sheet were fewer and larger than those of A0-80-500 sheet.

It is assumed that trans-crystal formation mechanism is closely related to a sheet forming method. When PP sheet is formed by a sheet forming machine, sheet is extruded with a high shear rate and a high shear stress at a skin layer according to the equation ((3))

$$\gamma = 6Q/Wt^2 \tag{3}$$

where γ is shear rate [s^{-1}], Q is quantity of flow [$m^3\ s^{-1}$], W is width of die [m], and t is clearance of die lip [m]. Since A0-80-500 sheet was formed at the quantity of 3.7×10^{-6} $m^3\ s^{-1}$ from the die width 0.2 m width and the clearance of die lip of 1×10^{-3} m, γ was calculated 111 s^{-1}. As PP molecular is extruded from die at high shear rate and cooled at low temperature before molecular was relaxed, it is assumed that skin layer with oriented molecular chain is formed and numerous trans-crystals were formed from the skin layer as the nuclei. Also, it is assumed that trans-crystals are easy to grow to the perpendicular direction to the surface, but are difficult to grow to the parallel direction to the surface because a lot of trans-crystals begin to grow from the skin layer at the same time and there is not enough area to grow to the parallel direction to the surface. On the other hand, it is assumed that there is almost no shear rate and no shear stress when the PP sheet was produced by a pressing machine. Since the skin layer with oriented PP molecular chain is not formed, there were few nuclei for the formation of trans-crystals. Therefore, deep and wide trans-crystals are easy to grow because there is an enough area not only to the perpendicular direction but also to the parallel direction to the surface. From these results, it is clarified that the PP molecular orientation in the skin layer gives a great influence on the formation of trans-crystals. It is concluded that trans-crystal formation is possible to control with the shear rate condition, that is to say, it is possible to control the crater formation.

CONCLUSION

It is clarified that nucleator gives a big influence on the formation of the crystal grains in the surface layer of PP sheet and on the formation of crater. α nucleators decrease the β crystal content K value with the added content of over 10 ppm, and make the size of crystal grain smaller and the number of it more. Whereas β nucleators increase the β crystal content without changing the crystal grain size with the added content of 100 ppm, they make the crystal grain size smaller with the content of 300 ppm. It was found that even when the crystal grain shape was equal, the crater shape differed if the melting point is different.

Crater was not formed on the BOPP films stretched from the sheet of which the skin layer with crystal grain was shaved and from the sheet in which β crystal still remained. Therefore, it is concluded that the existence of β crystal in the surface layer of PP sheet is not essential in order to produce craters on BOPP films, but crystal grains are necessary to form the craters. It was clarified that the crystal grain is trans-crystal and crater was formed from the aperture formed between the trans-crystals at the low stretching ratio from the observation by TEM. It was

Table II. Crystalline Structure of Piece Shaved from the Surface Layer of A0-80-300 Sheet from the Opposite Side of Chill-Roll

Depth of shaved piece (μm)	χ_c (%)	K
10-20	47.3	0.25
20-30	47.6	0.23
30-40	50.2	0.32

concluded that crater was formed by changing and deforming trans-crystal starting with the apertures between the trans-crystals. In addition, it was found that crater became larger and fewer on the BOPP film surface stretched from the PP sheet produced by a pressing machine than that of PP sheet produced by a sheet forming machine. This is caused by the larger and fewer trans-crystals on the PP sheet produced by a pressing machine because there were fewer shear stresses than the PP sheet produced by a sheet forming machine. From these results, it is concluded that the crater shape and number on BOPP films are influenced by the trans-crystals shape and number in the surface layer of PP sheet. Furthermore, it is concluded that the crater structure is possible to design as it is required by controlling the trans-crystal structure in the surface layer of PP sheet.

REFERENCES

1. Natta, G.; Gorradini, P. *Nuovo Cimento Suppl.* **1960**, *15*, 40.
2. Fujiyama, M.; Kawamura, Y.; Wakino, T.; Okamoto, T. *J. Appl. Polym. Sci.* **1988**, *36*, 1025.
3. Zhang, Y.; Xin, Z. *J. Polym. Sci. Part B: Polym. Chem.* **2007**, *45*, 590.
4. Keith, H. D.; Padden, F. J.; Walter, N. M.; Wickoff, H. W. *J. Appl. Phys.* **1959**, *30*, 1485.
5. Fujiyama, M.; Kawamura, Y.; Wakino, T.; Okamoto, T. *J. Appl. Polym. Sci.* **1988**, *36*, 985.
6. Yamaguchi, M.; Fukui, T.; Okamoto, K.; Sasaki, S.; Uchiyama, Y.; Ueoka, C.; *Polymer* **2009**, *50*, 1498.
7. Moitzi, J.; Skalicky, P. *Polymer* **1993**, *34*, 3168.
8. Farah, M.; Bretas, R. *J. Appl. Polym. Sci.* **2004**, *91*, 3528.
9. Nakamura, K.; Shimizu, S.; Umemoto, S.; Thierry, A.; Lotz, B.; Okui, N. *Polym. J.* **2008**, *40*, 915.
10. Koike, Y.; Cakmak, M. *Polymer* **2003**, *44*, 4249–4260.
11. Phillips, R. A.; Nguyen T. *J. Appl. Polym. Sci.* **2001**, *80*, 2400.
12. Sakauchi, K.; Uehara, H.; Yamada, T.; Obata, Y.; Takebe, T.; Kanai, T. *Polymer Processing Society Annual Meeting,* **2005**, p 21.
13. Kanai, T.; Matsuzawa, N.; Takebe, T.; Yamada, T. *Polymer Processing Society Regional Meeting Europe CD-ROM Abstracts*; **2007**.
14. Kanai, T.; Matsuzawa, N.; Yamaguchi, H.; Takebe, T.; Yamada, T. *24th Polymer Processing Society Annual Meeting CD-ROM Abstracts*; **2008**.
15. Kanai, T.; Takebe, T.; Matsuzawa, N.; Yamaguchi, H. *Asian Workshop on Polymer Processing Plenary Lecture*; **2009**.
16. Kanai, T.; Yonekawa, F.; Kuramoto, I. *17th Polymer Proceedings of the Society Annual Meeting Abstracts*; **2001**, p 17.
17. Kanai, T. *Seikei-Kakou* **2006**, *18*, 53.
18. Matsuzawa, N.; Kamatani, Y.; Kanai, T.; Yamada, T.; Sakauchi, K.; Uehara, H. *22th Polymer Processing Society Annual Meeting CD-ROM Abstracts*; **2006**.
19. Tamura, S.; Kuramoto, I.; Kanai, T. *Polym. Eng. Sci.* **2012**, *52*, 1383.
20. Fujiyama, M.; Kawamura, Y.; Wakino, T.; Okamoto, T. *J. Appl. Polym. Sci.* **1988**, *36*, 995.
21. Fujiyama, M.; Kawamura, Y.; Wakino, T.; Okamoto, T. *J. Appl. Polym. Sci.* **1988**, *36*, 1011.
22. Fujiyama, M.; Kawamura, Y.; Wakino, T.; Okamoto, T. *J. Appl. Polym. Sci.* **1988**, *36*, 1035.
23. Fujiyama, M.; Kawamura, Y.; Wakino, T.; Okamoto, T. *J. Appl. Polym. Sci.* **1988**, *36*, 1049.
24. Fujiyama, M.; Kawamura, Y.; Wakino, T.; Okamoto, T. *J. Appl. Polym. Sci.* **1988**, *36*, 1061.
25. Tamura, S.; Ohta, K.; Kanai, T. *J. Appl. Polym. Sci.* **2012**, *124*, 2725.
26. Funaki, A.; Kuratani, S.; Yamada, T.; Kanai, T. *Seikei-Kakou* **2011**, *23*, 299.
27. Tamura, S.; Takino, K.; Yamada, T.; Kanai, T. *J. Appl. Polym. Sci.* **2012**, *126*, E501.
28. Zambelli, A.; Locatelli, P.; Bajo, G.; Bovey, A. *Macromolecules* **1975**, *8*, 687.
29. Tuner-Jones, A.; Aizilewood, J. M.; Beckert, D. R. *Makromol. Chem.* **1964**, *75*, 134.
30. Natta, G.; Corradini, P.; Cesari, M.; *Rend. Accad. Naz. Lincei* **1957**, *22*, 11.